Polymer Chemistry

# Synthesis and Optoelectronic Properties of Benzodithiophene-Based Conjugated Polymer with Hydrogen Bonding Nucleobase Side Chain Functionality



| | |
|---|---|
| Journal: | *Polymer Chemistry* |
| Manuscript ID | PY-ART-07-2020-000972 |
| Article Type: | Paper |
| Date Submitted by the Author: | 06-Jul-2020 |
| Complete List of Authors: | Sabury, Sina; University of Tennessee Knoxville, Chemistry<br>Adams, Tyler; University of North Carolina at Charlotte, Chemistry<br>Kocherga, Margaret; University of North Carolina at Charlotte, Chemistry<br>Kilbey, S.; University of Tennessee, Chemistry<br>Walter, Michael; University of North Carolina at Charlotte, Chemistry |
| | |

# Synthesis and Optoelectronic Properties of Benzodithiophene-Based Conjugated Polymer with Hydrogen Bonding Nucleobase Side Chain Functionality

Sina Sabury,[1†] Tyler J. Adams,[2†] Margaret Kocherga,[2] S. Michael Kilbey II,[1,3]* Michael G. Walter,[2]*

[1] Department of Chemistry, University of Tennessee – Knoxville, Knoxville TN 37996

[2] Department of Chemistry, University of North Carolina – Charlotte, Charlotte NC 28223

[3] Department of Chemical & Biomolecular Engineering, University of Tennessee – Knoxville, Knoxville TN 37996.

[†] Authors contributed equally

* correspondence to Michael.Walter@uncc.edu or mkilbey@utk.edu

**Abstract:**

Fundamental properties of conjugated copolymers are sensitively linked to their constitution and features of their repeat unit design that govern assembly and organization across multiple length scales, ultimately impacting device performance. Herein we report the efficient synthesis and characterization, and optical, electrochemical and transport properties of complementary pairs of nucleobase-functionalized, fully conjugated copolymers based on benzo[1,2-b:4,5-b']-dithiophene (BDT) and 3-hexylthiophene (3hT), which is a quintessential low bandgap polymer. Stille cross-coupling polymerizations enable access to high molecular weight, alternating copolymers of modest dispersity containing pendant adenine or thymine groups in each repeating unit, which provide the capacity to direct molecular assembly. Variations in nucleobase type and design of

alkyl side chains on BDT units give rise to a strongly red-shifted absorbance onset for the copolymers containing thymine and adenine functionality in comparison to solution and dried films. Higher hole mobilities were also observed and attributed to the tendency of the nucleobase inclusion to heighten organization. The influence of the nucleobases on the organization is further revealed when thermal pre-treatment is used during film formation: Modest heating before casting the non-functionalized BDT-3hT copolymers leads to increases in the mobility, optical absorbance and fluorescence, while copolymers with adenine or thymine pendant groups do not show analogous improvements, suggesting that the nucleobases have promoted nanoscale organization, which is consistent with assessments of hydrogen bonding interactions. Given the structure-directing ability of nucleobases through hydrogen bonding, π-stacking, and complementary base pairing, these novel materials engender myriad opportunities to examine how specific molecular-level interactions that cue self-assembly affect optoelectronic properties and device-level performance.

## Introduction

Conjugated polymers have been used in numerous types of organic electronic devices, such as light-emitting diodes, field-effect transistors, photodetectors, and solar cells, as well as in applications like electrochromic windows and sensors, batteries and supercapacitors.[1-6] A rich variety of modifications to either the main chain or side chains have been utilized to enhance key performance attributes of conjugated polymers.[7-8] For instance, the incorporation of fused ring monomeric units such as carbazole, fluorene, and benzo[1,2-b:4,5-b']-dithiophene (BDT) are shown to extend the conjugation length, narrow the band gap, and thus increase the light absorbance limits.[7, 9-11] Diketopyrrolopyrrole (DPP)-based polymers show promising charge transport properties and application in organic electronics that emerges from enhanced interconnectivity of polymer chains due to DPP polar backbone.[12-13] Similarly, BDT-based polymers have received considerable attention, where modulating the constituents of the polymer backbone and adding electron withdrawing halogenated thienyl units to BDT have recently been shown to deepen HOMO levels of the donor-acceptor type polymers, which along with enhancements in planarity of the chain, lead to dramatic improvements in photovoltaic performance.[14-16]

Side chain engineering also is widely used to tailor the properties of conjugated polymers, oligomers, and small molecules with changes in functionality or design affecting the photophysical properties, solubility, phase separation, and intermolecular packing.[12, 17-23] Beyond varying the size or branch location in alkyl side chains,[24-26] as discussed by Bao et al., integrating ionic, polar, or other types of functionality within side chains provides a means to enhance optoelectronic properties and expand the applicability of conjugated polymers.[18] Within this pursuit, a handful of works have focused on functionalities that participate in hydrogen bonding. For example, Yao et

al. showed that when urea groups were present in side chains of DPP-based copolymers, higher hole mobilities were observed. This improvement was attributed to hydrogen bonding that enhanced ordering and increased domain sizes upon self-aggregation.[20] Ocheje et al. similarly showed that hydrogen bonding interactions provided by amide groups present in alkyl side chains of DPP-based conjugated polymers improved charge carrier mobility and nanoscale organization.[23] Hydrogen bonding interactions can also be used to organize small conjugated molecules, as shown by Lam et al.[27] Specifically, hydrogen bonding between carboxylic acid end groups on small molecules generated pseudo-conjugated polymer structures. With these self-organized pseudo-polymers, optimal device performance was achieved with as-cast films rather than thermally annealed samples.[27] In addition to reducing the reliance on thermal or solvent annealing and promoting molecular organization to enhance device performance, hydrogen bonding motifs also provide a viable strategy for surface immobilization and improving resistance to removal by solvent.[28-30] In total, these studies illustrate the close connections between improving optoelectronic properties of conjugated materials and structural features, as the ability to control structure across length scales ranging from molecular-level to mesoscopic not only affects chain conformation, packing, crystallization and domain sizes, but also impacts fundamental material properties and performance of organic electronic devices.[31-34]

Among the variety of structure-directing functionalities, nucleobases represent an intriguing type of functionality that may be used as an order-inducing motif.[35-36] Inspired by the potential for biomimicry, a well-known capacity for complementary, multi-dentate hydrogen bonding (as well as self-complementary hydrogen bonding), π-stacking, and the ability to bind cations, polymeric[17, 37-38] or oligomeric[39-40] materials containing nucleobase functionalities have been widely explored. For instance, nucleobases have been examined in applications such as

adhesives, self-healing materials, sensors, and templated arrays of nanoparticles, and they represent an emerging concept in organic electronic devices.[17, 41-47] Bäuerle and co-workers studied self-organization and functionality of π-conjugated oligomers appended with nucleosides and other biomolecules.[48-50] Guanine-functionalized oligothiophenes exhibited liquid crystalline and ion responsive behaviors due to the ability of guanine motifs to participate in self-complementary hydrogen bonding and form complexes with ions.[51] In the realm of polymeric materials, uracil, which is one of the four nucleobases of RNA, has been used as a pendant group in poly(alkyl thiophene) side chains. Cheng et al. used oxidative polymerizations or post-polymerization "click" reactions to create uracil-containing polythiophenes with different degrees of regioregularity and evaluated their impact as hole injection layers in OLED devices. Improvements in device characteristics were observed, with uracil-functionalized polythiophenes of low regioregularity displaying a significantly higher external quantum efficiency, brightness, and luminance efficiency compared either to devices without the hole injection layer or to devices made using a hole injection layer comprising high regioregular, uracil-tagged polythiophene (made by post-polymerization functionalization by an azide-alkyne click reaction). They attributed this improvement to physical connectivity between polythiophene chains brought on by self-complementary hydrogen bonding.[43] In a later study, Cheng et al. used Suzuki cross-coupling polymerizations to produce the first complementary pair of thymine- and adenine-functionalized polycarbazoles, and evaluated their impact as hole injection layers in OLEDs. While these copolymers were of modest molecular weight (~5 kDa), similar to the behavior exemplified in studies of uracil-functionalized poly(thiophene)s, physical cross-linking attributed to complementary adenine-thymine hydrogen bonding enhanced the performance of organic light-emitting diodes (OLEDs) relative to the performance of OLEDs constructed using poly(3,4-

ethylenedioxythiophene):poly(styrene sulfonate) as the hole injection layer.[52] Recently, Yang et al. harnessed the ability of nucleobases to bind metal ions, creating organic field effect transistors (OFETs) based on DPP/bithiophene alternating copolymers in which 5 mol% of DPP repeat units contained thymine-terminated, alkyl side chains. OFETs based on the resulting terpolymer, when first exposed to either $Pd^{2+}$ or $Hg^{2+}$ ions, demonstrated remarkable selectively toward CO or $H_2S$ gases, respectively. In addition, the terpolymers containing thymine at the terminus of the side chain displayed higher mobilities due to enhanced crystallinity, which was attributed to the directional H-bonding interactions between thymine groups.[17]

The combination of these themes of research – altering conjugated polymer type, changing side chain design, and adding structure-directing motifs – exemplify the premise of molecular engineering, which relies on deliberately manipulating molecular constituents and connectivity, and precisely encoding molecular-level interactions that operate at the nanoscale to generate new and useful material systems having enhanced properties and improved macroscopic performance. This represents a compelling challenge in the field of conjugated polymers, as organic semiconductors are marked by a strong interdependence between electronic and geometric structure,[53-54] and fundamental properties such as charge carrier mobility and excited state lifetimes, which are crucial to device performance, depend on efficient intermolecular contact, either in ordered structures or interconnected aggregates.[1, 12, 55-56] Moreover, interfacial properties,[24, 57] domain sizes,[58-59] composition,[11, 60] and connectivity[19] also play crucial roles.

Motivated by the premise of harnessing non-bonded physical interactions to influence inter-chain interactions in semiconducting conjugated polymers, in this study we describe the synthesis of well-defined alternating copolymers based on BDT and 3-hexylthiophene (3hT) in which the hexyl side chains are terminated with either thymine (Thy) or adenine (Ad) nucleobases

as pendant functionality. The BDT repeating units have either linear alkyl (dodecyl) or branched alkoxy (ethyl hexyloxy) side chains. In addition to the four nucleobase-modified copolymers, the analogous copolymers without nucleobases in the side chain are synthesized and studied in order to begin to elucidate the impact of nucleobase functionality on optical, electrochemical and photophysical properties in solution and thin films.

## Results and Discussion

### Copolymer synthesis and characterization

A series of high molecular weight alternating copolymers based on benzodithiophene (BDT) and 3-alkyl thiophene were synthesized by Stille cross-coupling, as shown in **Figure 1**. Within this series, the side chains on BDT were either dodecyl (**$BDT_d$**) or branched ethyl hexyloxy (**$BDT_{eho}$**) and hexyl side chains on thienyl repeating units were terminally functionalized with either adenine (**$3hT_{Ad}$**) or thymine (**$3hT_{Thy}$**) pendant groups. These variations give rise to four distinct alternating, fully conjugated polymers that are identified by their alternating repeating units: **$BDT_d$-$3hT_{Ad}$**, **$BDT_d$-$3hT_{Thy}$**, **$BDT_{eho}$-$3hT_{Ad}$**, and **$BDT_{eho}$-$3hT_{Thy}$**. In addition and for comparison purposes, two alternating copolymers of BDT and 3-hexylthiophene were also synthesized, and these are referred to as simply **$BDT_d$-3hT** and **$BDT_{eho}$-3hT**. Macromolecular size and dispersity of these six fully conjugated, alternating copolymers are presented in **Table 1**. Although we maintained synthesis conditions, including monomer concentration and catalyst loading, consistent across all samples, the alternating copolymers containing nucleobase functionalities were of lower molecular weight, likely due to limited solubility of the nucleobase-

functionalized polymer[61] as well as potential undesired catalyst-nucleobase interactions, which we described recently.[38]

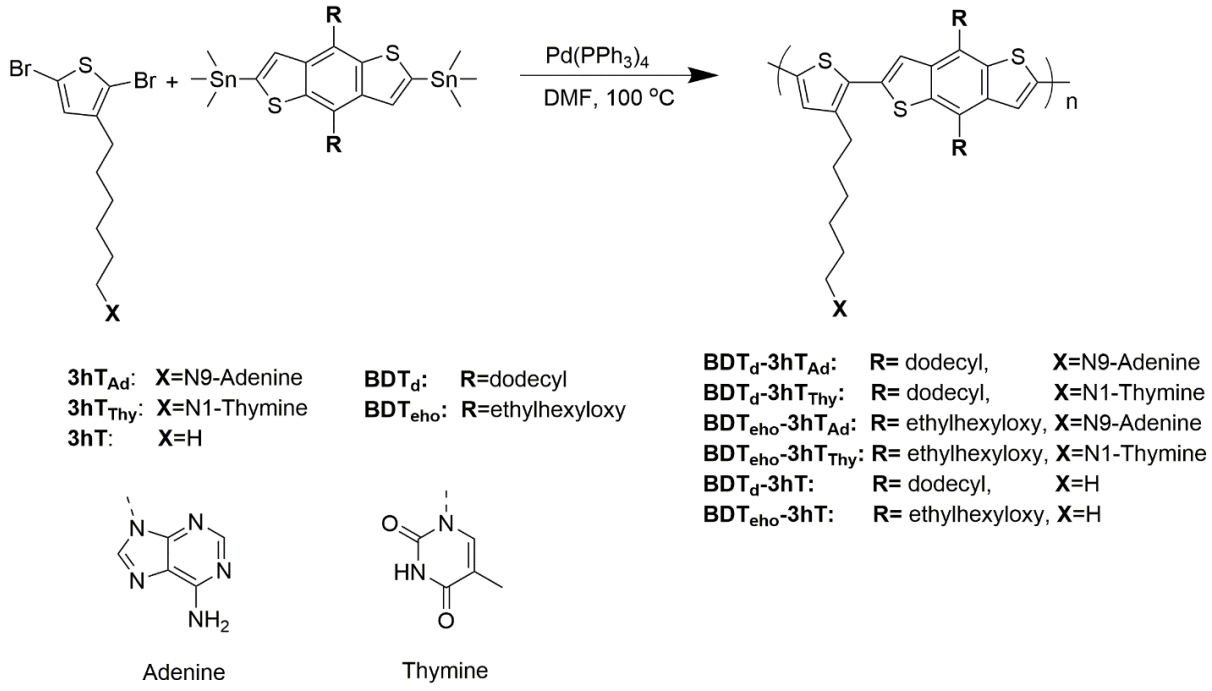


**Figure 1.** Synthesis scheme of BDT-3hT alternating, regiorandom copolymers prepared by Stille cross coupling polymerization. These are generally referred to as $\mathbf{BDT_R\text{-}3hT_X}$ copolymers, with the identity of R and X defined herein.

Although solubility issues are not uncommon with fully conjugated polymers, the presence of the nucleobases heightened these challenges: For example, Stille cross-coupling polymerization of 2,5-bis-(trimethylstannyl)thiophene with 2,5-dibromo-3-(6-adenine)hexylthiophene ($\mathbf{3hT_{Ad}}$) produced a polymer that was soluble only in hot DMF, rendering it impossible to characterize. Similarly, in the case of a semi-random terpolymer produced by Stille cross-coupling polymerization of 2,5-bis-(trimethylstannyl)thiophene, 2,5-dibromo-3,4-dihexylthiophene, and $\mathbf{3hT_{Ad}}$, only the material recovered after Soxhlet extraction with acetone could be redissolved

**Table 1. Characteristics of $BDT_R$-$3hT_x$ Alternating Copolymers.**

| Copolymer | $M_n$ (g $mol^{-1}$)[a] | Đ | Yield (%) | Nucleobase attachment |
|---|---|---|---|---|
| $BDT_d$-$3hT_{Ad}$ | 17,300 | 2.36 | 55 | N9 |
| $BDT_d$-$3hT_{Thy}$ | 16,000 | 2.40 | 88 | N1 |
| $BDT_{eho}$-$3hT_{Ad}$ | 11,300 | 1.50 | 64 | N9 |
| $BDT_{eho}$-$3hT_{Thy}$ | 19,900 | 1.55 | 85 | N1 |
| $BDT_d$-3hT | 45,000 | 1.43 | 53 | - |
| $BDT_{eho}$-3hT | 36,900 | 1.58 | 79 | - |

[a] measured by GPC; relative to PS standards.

and characterized by GPC (2900 g $mol^{-1}$, Đ = 1.2). As a result, **$BDT_d$** and **$BDT_{eho}$** were used as comonomers to help mitigate these solubility issues. While the data in **Table 1** clearly suggests that Stille polymerizations are effective for the synthesis of nucleobase-functionalized, fully conjugated copolymers, we found that if those copolymers were dried as part of a purification process, their redissolution was challenged. This phenomenon is also observed in self-aggregating colloidal dispersions, where slow solvent removal step promotes irreversible aggregations and thus results in a non-processable solid.[62] Inspired by efforts to mitigate aggregation driven by pi-stacking in graphene-polymer nanocomposites [63] and hydrogen bonding in pharmaceuticals [64] we developed a solution-based processing step to exchange the solvent from chloroform – the extraction solvent used in post-polymerization purification – to the desired, higher boiling-point

solvent, such as dioxane. By avoiding aggregation, the solvent transfer method proved to be effective for casting homogeneous and smooth thin films. To prepare samples for GPC, or $^1$H NMR analysis, after completing the solvent-transfer to dioxane, the samples were subjected to freeze-drying. Freeze-drying has been used to overcome irreversible aggregations in palygorskite which is a type of clay shown that organizes by strong hydrogen bonding interactions in the solid state.[65] Dioxane is an excellent choice for freeze-drying because of its accessible triple point (~ 11 °C). After freeze-drying, samples for analysis by GPC or $^1$H NMR spectroscopy were dissolved in THF or $CDCl_3$, respectively. We expect that our method of solvent transfer, which is shown in Figure S9, also will be applicable to other marginally-soluble or self-aggregating conjugated (or non-conjugated) polymeric materials.

All polymers exhibit high thermal stability, with **BDT$_d$**-based copolymers showing higher stability compared to **BDT$_{eho}$**-based copolymers. Unfunctionalized copolymers were more thermally stable than Ad-functionalized copolymers, which were more stable than Thy-functionalized copolymers. An extra feature in the degradation profile, ostensibly corresponding to loss of ethyl hexyloxy side chains, was observed in thermogravimetry studies of **BDT$_{eho}$**-based copolymers. (This occurred in the range of ~400 °C – 500 °C, representing ~10% weight loss; see *ESI* for all TGA results.) Although DSC measurements did not show evidence of a distinct glass transition, it is noted that similar behavior (no $T_g$ by DSC) has been reported for a variety of BDT-based conjugated polymers.[25, 66-69] Also, no crystallization peaks were observed in thermograms recorded by DSC for any of the 6 copolymers. This lack of crystallinity is attributed to regiorandom incorporation of 3hT repeating units and consistent with wide-angle x-ray scattering studies of thins films described later.

**Hydrogen bonding ability of nucleobase functionalities**

Self-complementary hydrogen bonding between nucleobase functionalities (Thy···Thy and Ad···Ad) have the potential to influence charge transport properties by altering the organization of the chains. $^1$H NMR studies were utilized to assess the hydrogen bonding ability and its strength of the pendant Ad and Thy groups, as it is known that these interactions can be observed by downfield shifts of the hydrogen atoms involved in the complementary interactions between the nucleobases.[70] A suite of approaches involving $^1$H NMR have been used previously to assess the chemical shift of hydrogens involved in H-bonding: self-complementary H-bonding interactions may be assessed through (i) variable temperature/constant concentration experiments or (ii) constant temperature/variable concentration experiments; while complementary interactions may be examined through (iii) guest-host titration studies.[71-73] Unfortunately, both types of direct $^1$H NMR monitoring to examine self-complementary H-bonding (methods I and ii) did not provide reliable or conclusive results due to the fact that the $^1$H NMR signals of the relevant protons are broadened in the polymeric materials and solubility range for **BDT$_R$-3hT$_{Thy/Ad}$** copolymers is limited. Similar complications were reported by Long et al. in their studies of acrylate copolymers functionalized by nucleobases.[70, 74] Thus, we adopted their approach of studying small molecules analogs in order to demonstrate that these fully conjugated, nucleobase-functionalized copolymers are capable of hydrogen bonding. In order to analyze the Thy···Thy and Ad···Ad interactions, we performed concentration-dependent $^1$H NMR study on the small molecules, adenine-N9-hexyl and thymine-N1-hexyl, in deuterated chloroform using concentrations ranging from 1 mM to 18 mM. As shown in **Figure 2a** for adenine-N9-hexyl (structure inset in **Figure 2b**), the $NH_2$ protons gradually shift downfield from 5.48 to 5.61 as the concentration was systematically increased from1 mM to 17 mM. Nonlinear regression analysis of the observed chemical shift, $\delta_{obs}$, of the

$NH_2$ protons resulted in the dimerization constant ($K_{dimer}$) of $K_{dimer,\ Ad\text{-}Ad} = 17\ M^{-1}$ for adenine-N9-hexyl. Similarly and as shown in **Figure 2c**, the signal from N3-H of thymine-N1-hexyl shifted downfield from 7.95 to 8.27 as the concentration was increased from 1 mM to 17 mM. Nonlinear regression analysis yielded a dimerization constant $K_{dimer,Thy\text{-}Thy} = 19\ M^{-1}$ for thymine-N1-hexyl (structure inset in **Figure 2d**). These values are in good agreement with reported values for nucleobase-containing molecules[75] and consistent with the idea that self-complementary Thy···Thy and Ad···Ad hydrogen bonds are weaker than Thy···Ad host-guest interactions. To assess this quantitatively, we performed titration experiment in which adenine-N9-hexyl was systematically added to thymine-N1-hexyl (concentration = 8 mM). As shown in Figure S18 (ESI), the measured chemical shift of the N3-H proton of thymine-N1-hexyl as a function of adenine-N9-hexyl was analyzed using the Benesi–Hildebrand model,[76] which yielded a host-guest association constant, $K_{HG} = 29\ M^{-1}$ in chloroform. The dimerization association constants resulting from these studies support the contention that side chain functionalities present in the conjugated copolymer lead to interbase hydrogen bonds.

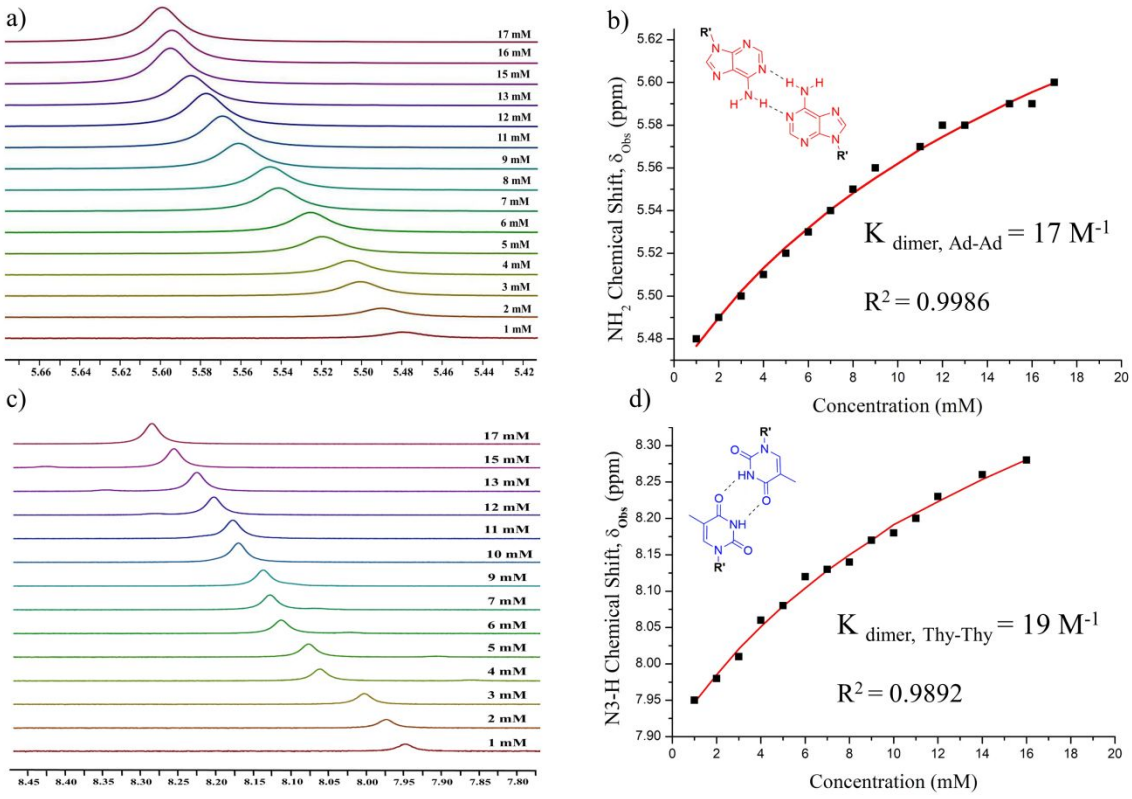


**Figure 2**. Small molecule analogs are used to assess self-dimerization of pendant nucleobase functionalities. Changes in the chemical shift of a) $NH_2$ and c) N3-H protons upon hydrogen bond dimerization as a function of concentration. Structures (R′ = hexyl) and self-association constants determined by nonlinear regression analysis are shown for b) adenine-N9-hexyl and d) thymine-N1-hexyl.

Insights about hydrogen bonding in the solid state were obtained by FTIR spectroscopy and by testing resistance of thin films to removal by solvent (solvent resistivity). It is reported that hydrogen bonding in alternating copolymers in the solid state can improve surface immobilization and solvent resistivity.[28-30] Thin films of **$BDT_R$-3h$T_X$** copolymers were fabricated on glass slides from dilute (1 mg/mL) chloroform solutions (3 samples for each copolymer). One sample was used as the control sample, one thin film was rinsed in chloroform twice for 20 s each time, and the third sample was sonicated in methanol for 20 minutes. (Methanol was used because it is a non-solvent that can participate in hydrogen bonding.) Images of the samples are shown in Table

S1 (ESI) with the results presented in **Figure 3.** Here, the relative solvent resistivity is derived by normalizing the optical absorbance intensity of solvent-exposed films by the absorbance intensity of the as-cast film. The results show that the control copolymers, **$BDT_d$-3hT**, and **$BDT_{eho}$-3hT,** have the lowest chloroform resistivity, with the former having only a 34% absorbance retention and the latter having only 15% absorbance retention after two chloroform rinses. Methanol resistivity did not show a specific pattern; however, it is notable that the nucleobase containing polymers showed moderate to high adhesion to glass slide where we tried to weaken hydrogen bonds using methanol. The adenine-functionalized copolymers showed highest solvent resistivity, with relative retention of absorbance intensities of 96% and 81% for **$BDT_d$-3h$T_{Ad}$** and **$BDT_{eho}$-3h$T_{Ad}$**, respectively, followed by the thymine-containing copolymers, **$BDT_d$-3h$T_{Thy}$** and **$BDT_{eho}$-3h$T_{Thy}$**, which retained 60% and 53% absorbance, respectively. Although it is prudent to refrain from direct quantitative comparisons because the Ad- and Thy-functionalized copolymers have different solubility toward chloroform (and presumably methanol), the essential point is that the ability of the nucleobase functionalized copolymers to interact through self-dimerization between groups is reflected in their relative solvent resistivity as compared to the non-functionalized copolymers.

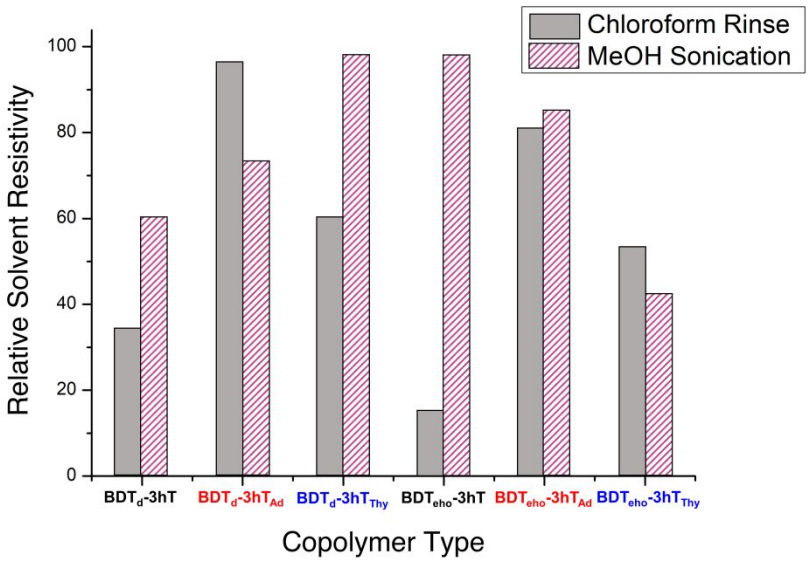


**Figure 3**. Relative solvent resistivity of **BDT$_R$-3hT$_X$** copolymers, which results from normalizing the optical absorbance intensity of solvent-exposed films by the absorbance intensity of the as-cast thin film samples.

In addition to somewhat qualitative assessments of solvent resistivity, additional information can be extracted by examining the intensity and shift in vibrational energies, as they are influenced by the hydrogen bonding environment.[77] FTIR spectra acquired from the **BDT$_{eho}$** and **BDT$_d$** series of copolymers dry powder samples are shown in Figure 3. Signatures due to C−H bond stretching of the side chains at 2855 cm$^{-1}$ and 2920 cm$^{-1}$ are more prominent for the **BDT$_d$-3hT$_X$** series than for the **BDT$_{eho}$-3hT$_X$** copolymers, as expected.[78] The presence of adenine in **BDT$_R$-3hT$_{Ad}$** copolymers is evident from the band at 1130 cm$^{-1}$, which is due to C−N bond stretching of the pyrimidine ring, and the mode at 1610 cm$^{-1}$ correlates to both C=C and C=N stretches of the six-membered ring of adenine. In addition, the broad peak above 3000 cm$^{-1}$ is attributed to stretching of N−H bonds (of the $NH_2$ group) and the mode at 1640 cm$^{-1}$ derives from a scissoring mode of the $NH_2$ of adenine.[79-81] The spectra for the **BDT$_R$-3hT$_{Thy}$** copolymers show characteristic bands due to the presence of thymine pendent groups. Specifically, broad bands due

to vibrational modes of C(2)=O, C(4)=O, and C(5)=C(6) are seen ~1680 $cm^{-1}$, a band arising from C(5)−$CH_3$ bending is present at 1380 $cm^{-1}$, and the endocyclic C−N stretching mode is seen at 1260 $cm^{-1}$.[80, 82]

Previous studies report that the peak positions of out-of-plane N−H bending in thymine and $NH_2$ wagging in adenine are most sensitive to the hydrogen bonding environment.[79-80] In the **$BDT_{eho}$-3h$T_{Thy}$**, and **$BDT_{d}$-3h$T_{Thy}$** copolymers, the out-of-plane N−H bending peaks are observed at 845 $cm^{-1}$ and 810 $cm^{-1}$, respectively, which is similar to that of N1-methylthymine in the solid state (845 $cm^{-1}$). It is worth noting that the out of plane N−H bending of single-crystalline N1-methylthymine is reported at 882 $cm^{-1}$,[80, 82] while the peak for isolated N(3)−H out-of-plane bending is estimated to be at 664 $cm^{-1}$.[79] Thus, the relative position of these modes suggest slightly stronger Thy···Thy hydrogen bonding in **$BDT_{eho}$-3h$T_{Thy}$** compared with **$BDT_{d}$-3h$T_{Thy}$**. For the **$BDT_{d}$-3h$T_{Ad}$** and **$BDT_{eho}$-3h$T_{Ad}$** copolymers, the $NH_2$ wagging band is observed at 646 $cm^{-1}$. $NH_2$ wagging band of N9-methyladenine in the solid state[81] and in single-crystalline[80] and matrix-isolated[79] forms are reported at 636 $cm^{-1}$, 690 $cm^{-1}$, and 530 $cm^{-1}$, respectively. The presence of this band at 646 $cm^{-1}$ confirms that there is relatively strong hydrogen bonding in the adenine containing alternating copolymers, despite differences in their molecular weight. Small but noticeable differences between ethyl hexyloxy- and dodecyl-solublized polymers were observed in their FTIR spectra. Slightly sharper peaks in the region of 1600-1800 $cm^{-1}$ and an extra shoulder peak are observed for the ethyl hexyloxy-substituted copolymers. These may be due to the ether groups of the side chains participating in hydrogen bonding, which has been reported for other alkoxyl groups.[83-84] It is hard to conclusively compare O···nucleobase hydrogen bonding and nucleobase···nucleobase hydrogen bonding due to presence of multiple absorbance bands in that

region from 1600-1800 $cm^{-1}$; however, it is expected that the ether-nucleobase hydrogen bonding interactions are weaker than hydrogen bonding between nucleobases.

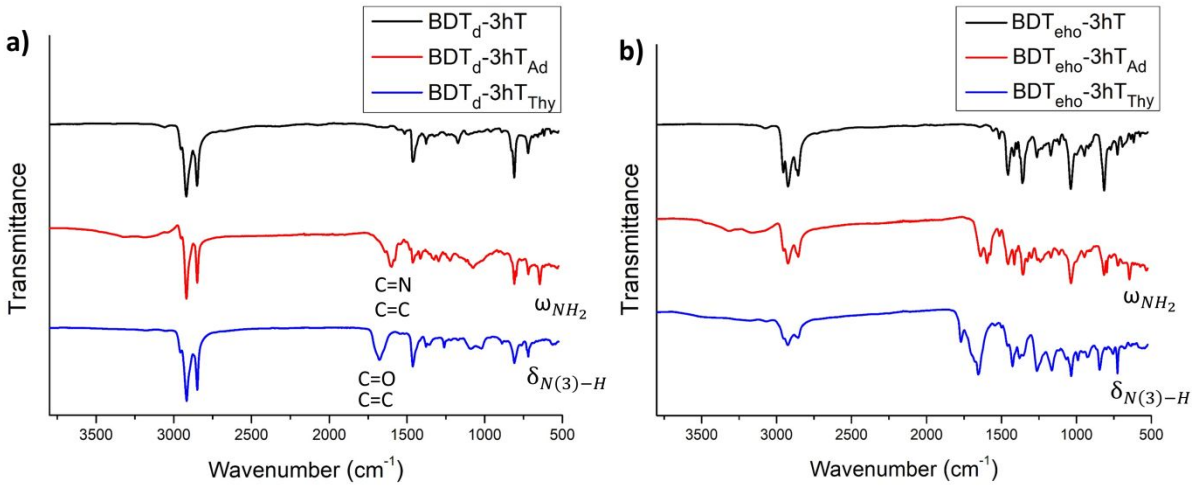


**Figure 4**. FTIR spectra of a) **BDT$_d$-3hT$_x$** and b) **BDT$_{eho}$-3hT$_x$** copolymers. Characteristic vibrational peaks for adenine and thymine groups in the region of 1600-1800 $cm^{-1}$ are labeled. Bands that are correlated to $NH_2$ wagging ($\omega_{NH_2}$) and N(3)−H out of plane bending ($\delta_{N(3)-H}$) are specified.

## Optical and electronic characterizations

As these alternating copolymers are novel, we used a variety of methods to assess the impact of the nucleobase functionality on the optical and electronic properties of the polymers. Results of UV-Vis and fluorescence spectroscopy for each of the copolymers in solution are shown in **Figure 5**. The unfunctionalized **BDT$_d$-3hT co**polymer shows an onset absorbance that is red-shifted by 50 nm from the **BDT$_{eho}$-3hT** copolymer, and this translates to a lower optical band gap energy as seen in **Table 2**. Both unfunctionalized copolymers exhibited very distinct absorbances with the **BDT$_d$-3hT** exhibiting three intense singlet transitions ($S_0$ – $S_N$, π - π*) from 475 – 600 nm, whereas the **BDT$_{eho}$-3hT** exhibited a strong absorbance peak at 500 nm and a shoulder at 550 nm. The absorption characteristics of the four functionalized copolymers show similar absorbance

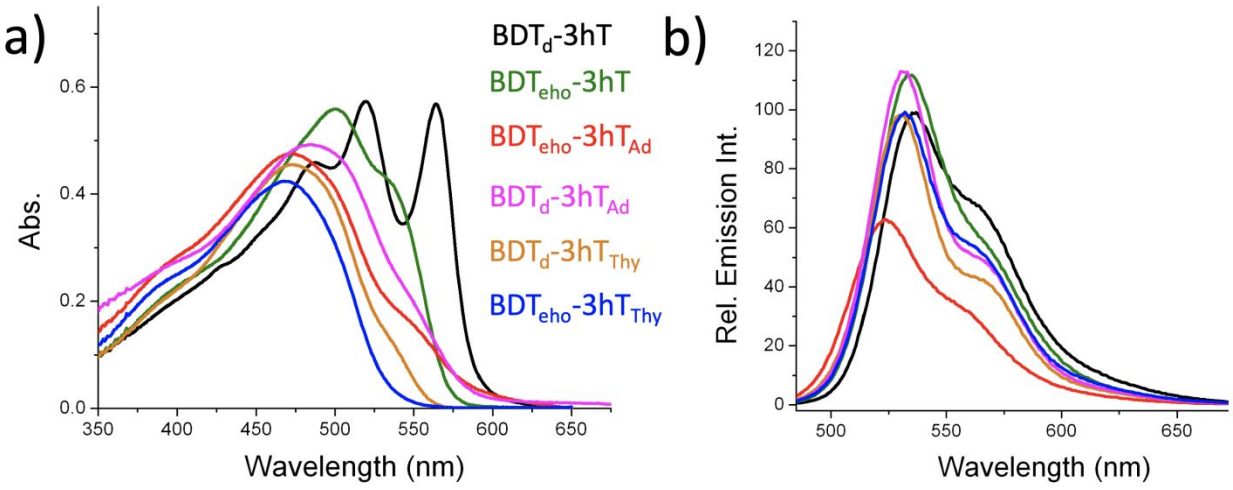


**Figure 5**. UV-Vis (a) and fluorescence (b) spectra of alternating copolymers in solution. Concentrations vary from 0.2-1.0 mM with emission spectra collected at 476 nm excitation. (Spectra were acquired using THF as the solvent, with the exception of **BDT$_d$-3hT$_{Ad}$**, which required a 1:1 mixture of DMSO and dichlorobenzene.) Line colors representing each copolymer are preserved between the two plots.

maxima ($\lambda_{max}$ = 450 – 500 nm) with absorbance onsets ranging from 550 – 600 nm, and are all blue-shifted from the unfunctionalized copolymers (**BDT$_{eho}$-3hT** and **BDT$_d$-3hT)**. As evident from **Figure 5**, the fluorescence spectrum of each of the alternating copolymers in dilute solution show nearly identical emission profiles. Fluorescent quantum yields were $\Phi_F$ = 0.16 and $\Phi_F$ = 0.19 for the unfunctionalized copolymers and ranged from $\Phi_F$ = 0.11 – 0.26 for the **BDT$_d$-3hT$_{Ad}$**, **BDT$_d$-3hT$_{Thy}$**, and **BDT$_{eho}$-3hT$_{Thy}$**. Although no clear trend in fluorescence yield was observed in solution, polymer conformation at low concentrations can impact the fluorescence intensity.[85] The addition of adenine pendant groups to the **BDT$_{eho}$-3hT** copolymer lowered the fluorescence yield to $\Phi_F$ = 0.11 whereas the addition of a thymine group (**BDT$_{eho}$-3hT$_{Thy}$**) increased the emission intensity to $\Phi_F$ = 0.23. For the **BDT$_d$-3hT** copolymers, the quantum yields increased for the addition of both adenine and thymine pendant groups. Overall, the radiative rates of emission, $k_s$ presented in **Table 2** (or fluorescence lifetime, $\tau$) are similar for all of the copolymers. Slightly

varied quantum yields and radiative rates may be related to emission quenching or polymer conformations in solution induced by the nucleobase groups.[86]

In the solid state, solution cast thin films exhibited a red-shifted absorbance spectrum, which is common with close packing and π - π interactions in conjugated molecular materials.[87] The red-shifted peak absorbance (compared to solution) for the unfunctionalized **$BDT_{eho}$-3hT** was small (Δλ = 4 nm), whereas the analogous copolymer having the thymine or adenine pendant groups resulted in a red-shifted absorbance spectrum of Δλ = 28 nm (**$BDT_{eho}$-3h$T_{Thy}$**) and Δλ = 36 nm (**$BDT_{eho}$-3h$T_{Ad}$**) (**Figure 6**). The variation between thin film and solution absorbance is

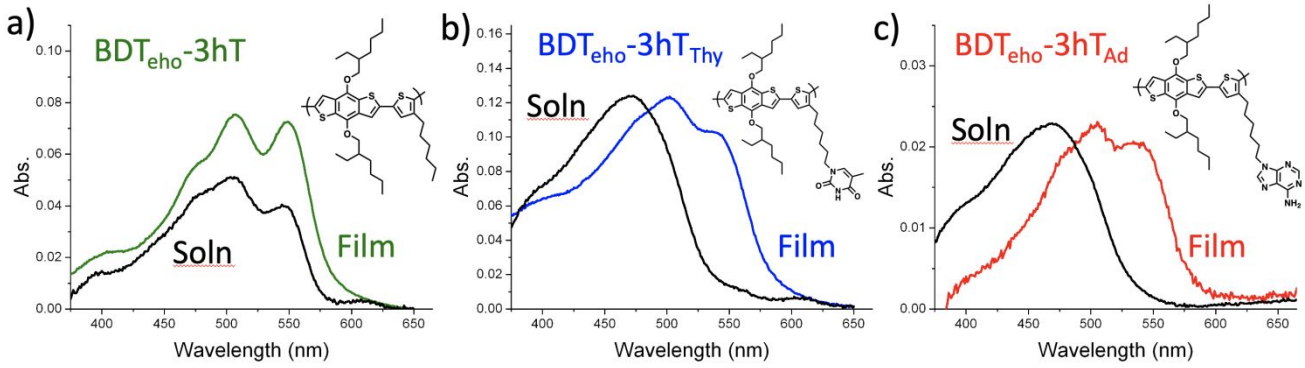


**Figure 6**. UV-vis absorbance spectra of alternating copolymers in solution (THF) and thin films drop-cast from THF for a) **$BDT_{eho}$-3hT**, b) **$BDT_{eho}$-3h$T_{Thy}$**, and c) **$BDT_{eho}$-3h$T_{Ad}$**.

even greater with the **$BDT_{d}$-3hT** functionalized polymers with a peak absorbance red-shift of Δλ = 47 nm for **$BDT_{d}$-3h$T_{Thy}$** and Δλ = 41 for **$BDT_{d}$-3h$T_{Ad}$**. (See data in Table 2 and Figure S19.) The optical band gaps and slight absorbance shift for the unfunctionalized **$BDT_{d}$-3hT** and **$BDT_{eho}$-3hT** are consistent with behaviors reported by Yang et al. for a donor-acceptor alternating copolymer consisting BDT (with didodecyl oxide side chains) and thiophene.[88] For both types of nucleobase functionalized copolymers (**$BDT_{d}$-3h$T_{Thy}$** and **$BDT_{eho}$-3h$T_{Thy}$**) there is a large spectroscopic impact, presumably as a result of its impact on thin film structure and polymer chain

packing.[17] Interestingly, the optical band gaps measured using the absorbance onset of the thin films are nearly identical for all of the functionalized and unfunctionalized copolymers (**Table 2**). This is encouraging and potentially useful for the development of polymer electronics, as it indicates that nucleobase pendant groups can be added to conjugated polymers for modulating their organization without strongly affecting their optical properties.

**Table 2. Photophysical Properties and Molecular Energy Levels of $BDT_R$-3h$T_x$ Copolymers**

| Copolymer | $\lambda_{max\text{-}soln}$ (nm)<br>$\lambda_{max\text{-}film}$ (nm) | $\Delta E_{gap\text{-}opt}$ (eV)[a] | $\Phi_F$[b] | $\tau$ (ps)<br>$k_s$ ($\times 10^8$ $s^{-1}$) | $E_{ox}$ (V)[c] | HOMO (eV)[d] | LUMO (eV)[d] |
|---|---|---|---|---|---|---|---|
| $BDT_{eho}$-3hT | 503<br>(507) | 2.12 | 0.16 | 855<br>(1.87) | 0.99 | -5.39 | -3.27 |
| $BDT_{eho}$-3h$T_{Ad}$ | 472<br>(505) | 2.13 | 0.11 | 979<br>(1.12) | 0.88 | -5.28 | -3.15 |
| $BDT_{eho}$-3h$T_{Thy}$ | 469<br>(502) | 2.11 | 0.23 | 855<br>(2.69) | 0.85 | -5.25 | -3.14 |
| $BDT_d$-3hT | 519<br>(516) | 2.10 | 0.19 | 897<br>(1.91) | 1.00 | -5.40 | -3.30 |
| $BDT_d$-3h$T_{Ad}$ | 477<br>(518) | 2.07 | 0.26 | 886<br>(2.94) | 0.79 | -5.19 | -3.12 |
| $BDT_d$-3h$T_{Thy}$ | 473<br>(520) | 2.09 | 0.22 | 828<br>(2.66) | 0.97 | -5.37 | -3.28 |

[a] Estimated from the UV-vis onset absorbance of the thin films
[b] Measured by comparison method using fluorescein standard
[c] Thin film electrochemical onset potentials are reported vs. SCE
[d] $E_{HOMO}$ (eV) = -($E_{ox\text{-}onset}$ + 4.4) eV, $E_{LUMO}$ calculated using $\Delta E_{gap\text{-}opt}$

Two different protocols were used with spin coating to further understand packing effects in thin films. One protocol involved preheating the solution and glass substrates to 60 °C before spin coating, while another used preheating at 120 °C. **BDT-3hT** thin film absorbance and

fluorescence (both **BDT$_{eho}$** and **BDT$_{d}$** derivatives) was higher when spin cast at 120 °C than films spin cast at 60 °C. The increased absorbance and emission were less in **BDT-3hT$_{Thy}$** derivatives, while **BDT-3hT$_{Ad}$** thin films changed very little when spin cast at 120 °C, compared to 60 °C (**Figure S20**). This enhancement in film thickness or advantageous polymer packing behavior is attributed to the ability of nucleobases to promote organization or improve chain packing. Unfortunately, grazing incidence wide-angle x-ray scattering (GIWAXS) showed minimal crystallinity in the spin cast thins films of each of the copolymers with 1-2 weak diffraction peaks observable in films cast at both temperatures. In general, processing the thin films of **BDT-3hT** copolymers (those without nucleobase functionality) at higher temperatures resulted in the greatest changes in spectroscopic intensity, which could be most readily observed in the emission spectra of **BDT$_{eho}$-3hT** and **BDT$_{d}$-3hT** copolymers, which are presented in **Figure S20** along with corresponding results from the nucleobase-functionalized copolymers.

Annealing the polymer thin films was also studied to deliver additional insight into packing changes due to hydrogen bonding interactions. When the films were annealed at 120 °C for 15 min, the absorbance spectra (**Figure S21**) for **BDT$_{eho}$-3hT**, **BDT$_{eho}$-3hT$_{Thy}$**, and **BDT$_{d}$-3hT$_{Thy}$** only changed slightly, whereas the absorbance of the adenine-functionalized copolymers, **BDT$_{eho}$-3hT$_{Ad}$** and **BDT$_{d}$-3hT$_{Ad}$**, decreased more. The non-nucleobase functionalized **BDT$_{d}$-3hT** showed the largest change in absorbance when annealed, particularly in the number of peaks, which changed from 2 strong peaks to one broad absorbance band. Based on these results, we conclude that preheating the co-polymer solutions prior to solution casting had a larger effect on the packing and morphology of the polymer films than annealing after spin casting.

The electrochemical oxidative properties of all the copolymers were evaluated as dried films on glassy carbon electrodes. As seen in **Figure 7**, electrochemical characterization shows the

onset of oxidation at 1.0 vs. SCE for the **$BDT_d$-3hT** and **$BDT_{eho}$-3hT** unfunctionalized copolymers respectively (**Table 2**). The addition of adenine and thymine pendant groups to the **$BDT_{eho}$-3hT** copolymer, shifts the onset of oxidation to more negative potentials, with a prominent strong oxidation peak indicating the presence of the nucleobases. The parent, non-nucleobase copolymer with (**$BDT_{eho}$-3hT**) had an oxidation onset of 0.99 V vs. SCE, which decreased with the addition of the adenine pendant group (**$BDT_{eho}$-3h$T_{Ad}$**) to 0.88 V vs. SCE and 0.85 V vs. SCE for thymine containing copolymers (**$BDT_{eho}$-3h$T_{Thy}$**). In the case of dodecyl side chain copolymers, the parent copolymer (**$BDT_d$-3hT**) had an oxidation onset of 1.00 V vs. SCE, which decreased to 0.97 V vs. SCE for **$BDT_d$-3h$T_{Thy}$** and 0.79 V vs. SCE for **$BDT_d$-3h$T_{Ad}$**. This observation agrees with previous reports of electrochemical oxidation of adenine and thymine.[89] The **$BDT_d$-3h$T_{Ad}$** and **$BDT_d$-3h$T_{Thy}$** copolymers also show a more negative oxidation onset than the non-nucleobase parent copolymer; however, the adenine and thymine oxidation waves are hidden by the strong oxidation of BDT and thiophene heterocycles present in the backbone.

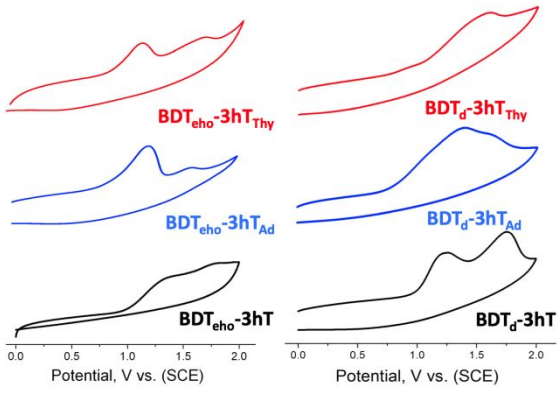


**Figure 7**. Cyclic voltammograms (electrochemical oxidative characterization) of alternating copolymers (dry films run in 0.1 M TBAP $CH_3CN$, 100 mV $s^{-1}$).

The charge transport properties of the copolymers were examined by solution processing thin films in hole-only devices for measuring the space charge limited current (SCLC) regime.[53] Devices consisted of spin coating the dissolved alternating copolymers onto PEDOT:PSS coated patterned ITO electrodes followed by thermal evaporation of a gold top contact. Due to variations in solubility, each copolymer required a particular solvent (or blend of solvents) to obtain uniform thin films. Film thicknesses measured by AFM were 8-38 nm, and these thicknesses agreed with model films produced on silicon wafers that were measured by spectroscopic ellipsometry.

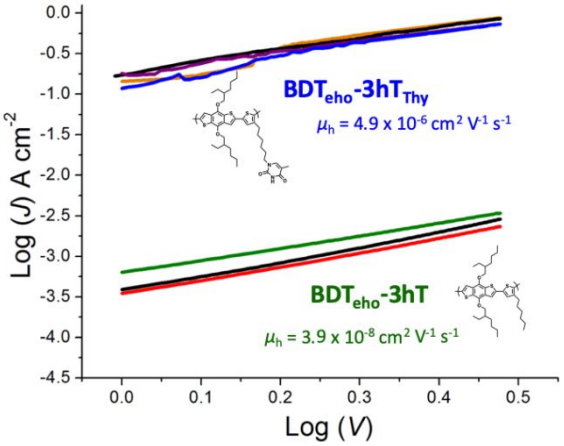


**Figure 8**. Hole mobility (Log $J$ – Log $V$) for **BDT$_{eho}$-3hT** and **BDT$_{eho}$-3hT$_{Thy}$** copolymer devices (ITO/PEDOT:PSS/BDT$_R$-3hT$_x$/Au) with structures and average mobilities inset in the plot. The individual lines correspond to tests of replicate devices. (Film thicknesses were 38 nm for **BDT$_{eho}$-3hT** and 30 nm for **BDT$_{eho}$-3hT$_{Thy}$**.)

Charge mobility, $\mu_h$, for the BDT copolymers were determined from the slope of the current density ($J$) versus applied potential ($V_a$) and fit to the simplified Mott-Gurney equation:

$$J = \frac{9}{8}\varepsilon\varepsilon_0\mu_h\frac{V_a^2}{L^3} \quad (1)$$

In this expression, $L$ is the measured polymer film thickness, $\varepsilon_0$ is the absolute permittivity and relative permittivity taken as $\varepsilon = 3$. A representative plot, expressed as log $J$ versus log $V$, is presented as **Figure 8**, which compares the behavior of **BDT$_{eho}$-3hT** and **BDT$_{eho}$-3hT$_{Thy}$**. The devices show slopes ranging from 1.4 to 2.3 in close agreement with SCLC charge mobility model.[90] For each copolymer, an average hole mobility derived from measurements of three to six device mobilities is reported in **Table 3**. Unfunctionalized **BDT$_{eho}$-3hT** showed the lowest hole mobility with little device-to-device variation and an average hole mobility of $3.9 \times 10^{-8}$ cm$^2$ V$^{-1}$ s$^{-1}$. Higher mobilities were observed for the unfunctionalized dodecyl-functionalized BDT copolymer, **BDT$_d$-3hT**, which displayed an average hole mobility of $7.1 \times 10^{-6}$ cm$^2$ V$^{-1}$ s$^{-1}$. Although molecular weight can have a significant impact on mobility, polymer chain packing is also a strong contributing factor for conjugated polymeric materials.[91] The hole mobility for **BDT$_d$-3hT** is similar to values previously reported for BDT-based polymers.[92] A significant enhancement of hole mobility was shown with the addition of nucleobases for the **BDT$_{eho}$-3hT** copolymers. The parent, non-nucleobase **BDT$_{eho}$-3hT** yielded a hole mobility of $\mu_h = 3.9 \times 10^{-8}$ cm$^2$ V$^{-1}$ s$^{-1}$, but adenine pendant group copolymer (**BDT$_{eho}$-3hT$_{Ad}$**) increased the hole mobility to $\mu_h = 1.8 \times 10^{-7}$ cm$^2$ V$^{-1}$ s$^{-1}$, while thymine pendant group copolymer (**BDT$_{eho}$-3hT$_{Thy}$**) yielded even higher hole mobility of $\mu_h = 4.9 \times 10^{-6}$ cm$^2$ V$^{-1}$ s$^{-1}$. The dodecyl-functionalized BDT copolymers had similar hole mobilities of $\mu_h = 7.1 \times 10^{-6}$ cm$^2$ V$^{-1}$ s$^{-1}$ for **BDT$_d$-3hT,** $\mu_h = 6.1 \times 10^{-6}$ cm$^2$ V$^{-1}$ s$^{-1}$ for **BDT$_d$-3hT$_{Ad}$** and $\mu_h = 1.5 \times 10^{-6}$ cm$^2$ V$^{-1}$ s$^{-1}$ for **BDT$_d$-3hT$_{Thy}$**. Although the nucleobase functionalized copolymers have slightly lower hole mobilities than the parent **BDT$_d$-3hT**, they are also one-third the molecular weight, as seen in **Table 1**. This molecular weight difference may offset the impact of the nucleobase-induced organization.

The mobility enhancements observed with **$BDT_{eho}$-3h$T_{Thy}$** and **$BDT_{eho}$-3h$T_{Ad}$** correlate with close and well-organized packing, which has been shown to greatly improve charge mobility in thymine-containing conjugated polymers.[17] The dodecyl side chain of the **$BDT_{d}$-3h$T_{Thy}$** may influence the copolymer stacking such that the probability of H- bonding interactions between

**Table 3. Charge (Hole) Mobility Measurements of $BDT_R$-3h$T_x$ Alternating Copolymers**

| Copolymer | $\mu_h$ ($cm^2\ V^{-1}\ s^{-1}$)[a] | $\mu_h$ ($cm^2\ V^{-1}\ s^{-1}$)[b] | Nucleobase attachment |
|---|---|---|---|
| **$BDT_{eho}$-3hT** | $3.9 \times 10^{-8} \pm 1.9 \times 10^{-8}$ | $3.8 \times 10^{-6} \pm 1.9 \times 10^{-6}$ | - |
| **$BDT_{eho}$-3h$T_{Ad}$** | $1.8 \times 10^{-7} \pm 3.1 \times 10^{-8}$ | $1.0 \times 10^{-7} \pm 2.6 \times 10^{-9}$ | N9 |
| **$BDT_{eho}$-3h$T_{Thy}$** | $4.9 \times 10^{-6} \pm 6.5 \times 10^{-6}$ | $1.2 \times 10^{-6} \pm 7.3 \times 10^{-7}$ | N1 |
| **$BDT_{d}$-3hT** | $7.1 \times 10^{-6} \pm 4.1 \times 10^{-7}$ | $7.7 \times 10^{-7} \pm 2.3 \times 10^{-7}$ | - |
| **$BDT_{d}$-3h$T_{Ad}$** | $6.1 \times 10^{-6} \pm 6.6 \times 10^{-7}$ | $5.2 \times 10^{-6} \pm 5.7 \times 10^{-6}$ | N9 |
| **$BDT_{d}$-3h$T_{Thy}$** | $1.5 \times 10^{-6} \pm 4.7 \times 10^{-7}$ | $2.5 \times 10^{-6} \pm 9.6 \times 10^{-7}$ | N1 |

[a] average mobility of three to six devices (device configuration **ITO/PEDOT:PSS/$BDT_R$-3h$T_x$/Au**) when **$BDT_R$-3h$T_x$** was spin cast at 60 °C.

[b] average mobility of three to five devices (device configuration **ITO/PEDOT:PSS/$BDT_R$-3h$T_x$/Au**) when **$BDT_R$-3h$T_x$** was spin cast at 120 °C.

nucleobases on adjacent copolymer chains is reduced, and therefore lowers organization and free-charge carrier conduction. Taken in aggregate, these results demonstrate a slightly more intricate

overall picture of nucleobase inclusion on organization and interactions of conjugated polymers, which along with the robust and generally facile syntheses, provides opportunities to further tune their optoelectronic properties using subtle structural variations through side chain engineering.

Finally, to examine whether enhancing the solubility and breaking interbase hydrogen bonding affected mobility, we increased the temperature to heat the solutions before casting from 60 °C to 120 °C. As seen in Table 3, the hole mobility for **BDT$_{eho}$-3hT** increased by two orders of magnitude while the hole mobilities of the **BDT$_{eho}$-3hT$_{Ad}$** and **BDT$_{eho}$-3hT$_{Thy}$** copolymers were minimally affected. Considering that heating was necessary for the **BDT$_{eho}$-3hT** to achieve mobilities consistent with devices made using **BDT$_{eho}$-3hT$_{Thy}$**, one striking conclusion that can be inferred from these behaviors is that thymine groups in the side chains can improve the morphology or nanoscale organization in a manner similar to thermal annealing. In the case of dodecyl-functionalized copolymers, the hole mobility measured for the non-nucleobase containing **BDT$_{d}$-3hT** copolymer decreased when the 120 °C spin coating protocol was implemented, while the mobilities measured for films made from the **BDT$_{d}$-3hT$_{Ad}$** and **BDT$_{d}$-3hT$_{Thy}$** were minimally affected, suggesting better organization stability due to interbase interactions.

## Conclusions

Stille cross-coupling polymerizations provide access to complementary pairs of donor-acceptor conjugated copolymers based on BDT and 3-alkyl thiophenes in which side chains contain adenine or thymine functionalities. The facility of the synthetic approach engenders opportunities to examine links between copolymer design, self-complementary and complementary H-bonding interactions, and π-stacking interactions on fundamental material

properties and performance. Evidence from a variety of studies on small molecules and conjugated polymers demonstrate that nucleobase functionalities can have significant effects on polymer stacking and solid-state electronic properties, with vibrational spectroscopy and solvent resistivity studies demonstrating inter-nucleobase hydrogen bonding in the solid state. The observation of enhancements in free charge carrier mobility has been reported previously, and we have also observed this phenomenon with adenine and thymine pendant groups attached to a novel BDT-containing conjugated copolymer having ethylhexoxy solubilizing side chains. The dodecyl-functionalized BDT copolymers also suggest this phenomenon, since the adenine and thymine nucleobase containing copolymers have hole mobilities similar to the parent non-nucleobase containing copolymer, even though they are one-third the molecular weight. Both results align with the degree of red-shifted absorbance onset observed when comparing solution and dried films, ultimately, providing early clues of copolymer organization that is influenced by inter-base hydrogen bonding in the adenine- and thymine-functionalized copolymers. Hole mobility of the polymers with nucleobase pendant groups are less dependent on the processing and thermal treatments, a behavior that also is attributed to inter-base hydrogen bonding in the solid state. These studies also suggest that there is a sensitive interplay between the strength, type, and number of non-bonded intermolecular interactions present in these copolymers. Additionally, this study provides spectroscopic clues of fluorescence quenching by an adenine pendant group, and the onset of electrochemical oxidation of the nucleobase pendant groups at lower potentials than the copolymer primary chain. Taken together, these materials show a range of exciting properties most notably, moderate hole mobilities and strong light absorbing and emission properties, which are useful for organic photovoltaic and light-emitting diode molecular electronic applications.

Moreover, they offer the potential to tease apart connections between molecular design, organization, and properties.

## Experimental Section

*Synthesis of Nucleobase-functionalized Monomers.* Nucleobase containing comonomers, 2,5-dibromo-3-(6-adenine)hexyl-thiophene, **3hT$_{Ad}$**, and 2,5-dibromo-3-(6-thymine)hexylthiophene, **3hT$_{Thy}$**, were synthesized from 3-(6-bromohexyl)thiophene by lithiation of 3-bromothiophene and subsequent addition of 1,6-dibromohexane, using procedures described in literature.[93] This monomer then was brominated following well known procedures to produce 2,5-dibromo-3-(6-bromohexyl) thiophene.[93] After isolation and purification, nucleobases (either adenine or thymine) were attached to 2,5-dibromo-3-(6-bromohexyl)thiophene by alkylation conditions,[94] thereby yielding either **3hT$_{Ad}$** or **3hT$_{Thy}$**. Complete synthetic details and results of $^1$H NMR and mass spectrometry are provided in the *Electronic Supplementary Information*.

*Copolymer Synthesis*. As depicted in **Figure 1**, two different bis(stannylated)-BDT monomers with either dodecyl or 2-ethylhexyloxy side chains were used along with **3hT$_{Ad}$** or **3hT$_{Thy}$** to produce four different nucleobase-functionalized alternating copolymers, **BDT$_d$-3hT$_{Ad}$**, **BDT$_d$-3hT$_{Thy}$**, **BDT$_{eho}$-3hT$_{Ad}$**, and **BDT$_{eho}$-3hT$_{Thy}$**. In addition, non-functionalized homologues, **BDT$_d$-3hT** and **BDT$_{eho}$-3hT,** were synthesized using Stille cross coupling polymerization of 2,5-dibromo-3-hexylthiophene with either **BDT$_d$**, and **BDT$_{eho}$**. Complete synthetic details and results of $^1$H NMR and gel permeation chromatography (GPC) characterizations are provided in the *ESI*.

*Thermal Characterizations*. Thermal stability of the polymers was determined using TA Instruments Q50 Thermogravimetric Analyzer (TGA) in an inert atmosphere of $N_2$ by ramping

from room temperature to 800 °C at a heating rate of 20 °C $min^{-1}$. For TGA measurements, the analytes were loaded in a platinum pan. Thermal properties were examined by differential scanning calorimetry (DSC) using a TA instruments Q-2000 DSC and a protocol consisting of a heat–cool–heat cycle from 50 °C to 270 °C with a heating rate of 10 °C $min^{-1}$ and a cooling rate of 10 °C $min^{-1}$ under an inert $N_2$ atmosphere. Samples (~5 mg) were sealed in standard aluminum pans.

*Photophysical Measurements*. Absorbance and fluorescence measurements were performed by making micromolar solutions of the polymers in tetrahydrofuran (THF). Molar absorbtivity of **$BDT_d$-3$hT_{Ad}$** was measured in 1:1 DMSO:1,2-dichlorobenzene. This also includes fluorescence quantum yield and molar absorptivity measurements. Thin films for UV-vis measurements were prepared by drop-casting from THF solutions. These measurements were performed using a Varian Cary Bio 300 UV-vis spectrophotometer and a Shimadzu RF-5301PC spectrofluorophotometer.

*Electrochemistry.* The oxidation of all 6 copolymers were determined by drop-casting each polymer onto a glassy carbon working electrode. Toluene was used to make films of **$BDT_{eho}$-3hT** and **$BDT_{eho}$-3$hT_{Thy}$**, chloroform was used for **$BDT_{eho}$-3$hT_{Ad}$**, chlorobenzene was used for **$BDT_d$-3hT** and **$BDT_d$-3$hT_{Thy}$**, and THF was used for **$BDT_d$-3$hT_{Ad}$**. A platinum flag counter electrode was used with a saturated calomel reference electrode in a 0.1 M tetrabutylammonium hexafluorophosphate in acetonitrile solution. The copolymers are not soluble in acetonitrile, so all of the copolymers remained on the working electrode. After purging the solution with argon for 5 min, each copolymer thin film was scanned 0 to 2 V at a scan rate of 100 mV/s. Three cycles were performed each time to prove that all the deposited polymer was oxidized after one cycle. When the second and third cycles were performed, the oxidation peak(s) disappeared. When scanned -2 to 2 V, the polymers were irreversibly oxidized.

*Device Preparation and Hole Mobility Measurements:* Patterned ITO glass (6 pixel) substrates from Ossila were cleaned by sonicating in DI water for 15 min, acetone for 15 min, then isopropyl alcohol for 15 minutes. Substrates were dried with nitrogen and treated in a UV/ozone ProCleaner for 10 min before PEDOT:PSS (Heraeus Clevios™ AI 4083) was applied by spin coating. Solution preparation and spin coating were performed under ambient conditions. The PEDOT:PSS (10 nm) was spin coated at 5000 RPM for 50 seconds with 90 μL using a Chemat Technology KW-4A spin coater. The ITO edge contacts were wiped off before annealing at 125 °C for 15 minutes. The **$BDT_R$-3h$T_X$** copolymers were spin coated on top of the PEDOT:PSS. **$BDT_{eho}$-3hT** was spin coated at 2000 RPM for 20 seconds with 45 μL from a 15 mg/mL 1,2-dichlorobenzene solution that was heated to 60 °C. **$BDT_d$-3hT** was dissolved in 1,2-dichlorobenzene at 10 mg/mL and spin coated with 90 μL at 5000 RPM for 50 seconds, after being heated to 60 °C. The **$BDT_{eho}$-3h$T_{Ad}$** and **$BDT_d$-3h$T_{Ad}$** polymers were spin coated at 2000 RPM for 50 seconds using 45 μL of 5 mg/mL solutions with 1,2-dichlorobenzene/DMSO (1/1 by volume). **$BDT_{eho}$-3h$T_{Thy}$** and **$BDT_d$-3h$T_{Thy}$** were spin coated from 10 mg/mL 1,2-dichlorobenzene/THF (1/1 by volume) at 5000 RPM for 50 seconds with 90 μL after being heated at 60 °C. When testing heating protocols, all devices were spin cast at 2000 RPM for 50 seconds using 45 μL of solution, with heating of the solution and substrates to either 60 °C or 120 °C. **$BDT_{eho}$-3hT** and **$BDT_d$-3hT** were dissolved in 1,2-dichlorobenzene at 10 mg/mL. The **$BDT_{eho}$-3h$T_{Ad}$** and **$BDT_d$-3h$T_{Ad}$** were spin coated using 5 mg/mL solutions with a mixed solvent of 1,2-dichlorobenzene/DMSO (1/1 by volume). **$BDT_{eho}$-3h$T_{Thy}$** and **$BDT_d$-3h$T_{Thy}$** were dissolved in 1,2-dichlorobenzene/THF (1/1 by volume) at 10 mg/mL. The multilayer devices (ITO glass/PEDOT:PSS/**$BDT_R$–3h$T_X$** copolymer) were then capped with a gold contact through thermal evaporation using a MB-EVAP system inside an MBRAUN glovebox. The gold films were deposited under high vacuum ($10^{-6}$ mbar) and the

thickness was controlled with a SQC-310C Deposition Controller. The gold was evaporated from a tungsten boat at a rate of approximately 1 Å $s^{-1}$. During deposition, the samples were rotated at 15 RPM and the source-to-film distance was 28 cm. A push-fit test board for pixelated anode substrates from Ossila was used with a Keithley 2602 A System SourceMeter® to measure $J - V$ curves.

## Acknowledgements

SS and SMK acknowledge partial support of this work from the National Science Foundation (Award No. 1512221). Early stages of this work derive from efforts supported by the Army Research Office (Agreement #W911NF-14-100153) and from the Laboratory Directed Research and Development Program of Oak Ridge National Laboratory, managed by UT-Battelle, LLC. MGW acknowledges support from the Nanoscale Science Ph.D. program and the Department of Chemistry at UNC Charlotte. MGW and SMK gratefully acknowledge thin film copolymer measurements provided by Dr. Tino Hofmann and Yanzeng Li of the Center for Optoelectronics and Optical Communications at UNC Charlotte, and Eric Williams and Morgan Stefik (University of South Carolina) for help with GIWAXS data collection.

## Conflicts of Interest

There are no conflicts to declare.

**Electronic Supplementary Information**

Details of monomer and polymer synthesis; results of copolymer characterization by $^{1}$H NMR, GPC, thermogravimetry and differential scanning calorimetry; details of solvent transfer method; solvent resistivity test images; photophysical properties of copolymers in solution and in thin films and assessment of Ad-Thy association constant in chloroform solution are provided in Supplementary Information. This material is available free of charge via the Internet at http://pubs.rsc.org.

**ORCIDs**

Sina Sabury: 0000-0003-0347-7405

Tyler J. Adams: 0000-0001-9759-8106

Margaret Kocherga: 0000-0002-7623-4829

Michael G. Walter: 0000-0002-9724-265X

S. Michael Kilbey II: 0000-0002-9431-1138

## References


1. Holliday, S.; Donaghey, J. E.; McCulloch, I., Advances in charge carrier mobilities of semiconducting polymers used in organic transistors. *Chem. Mater.* **2013,** *26* (1), 647-663.
2. Xie, G.; Luo, J.; Huang, M.; Chen, T.; Wu, K.; Gong, S.; Yang, C., Inheriting the Characteristics of TADF Small Molecule by Side-Chain Engineering Strategy to Enable Bluish-Green Polymers with High PLQYs up to 74% and External Quantum Efficiency over 16% in Light-Emitting Diodes. *Adv. Mater.* **2017,** *29* (11), 1604223.
3. Wu, Z.; Zhai, Y.; Kim, H.; Azoulay, J. D.; Ng, T. N., Emerging Design and Characterization Guidelines for Polymer-Based Infrared Photodetectors. *Acc. Chem. Res.* **2018,** *51* (12), 3144-3153.
4. Xie, J.; Gu, P.; Zhang, Q., Nanostructured conjugated polymers: toward high-performance organic electrodes for rechargeable batteries. *ACS Energy Lett.* **2017,** *2* (9), 1985-1996.
5. Liao, Y.; Wang, H.; Zhu, M.; Thomas, A., Efficient Supercapacitor Energy Storage Using Conjugated Microporous Polymer Networks Synthesized from Buchwald–Hartwig Coupling. *Adv. Mater.* **2018,** *30* (12), 1705710.
6. Zhang, S.; Ye, L.; Hou, J., Breaking the 10% Efficiency Barrier in Organic Photovoltaics: Morphology and Device Optimization of Well-Known PBDTTT Polymers. *Adv. Energy Mater.* **2016,** *6* (11), 1502529.
7. Zhou, H.; Yang, L.; You, W., Rational design of high performance conjugated polymers for organic solar cells. *Macromolecules* **2012,** *45* (2), 607-632.
8. Colladet, K.; Fourier, S.; Cleij, T. J.; Lutsen, L.; Gelan, J.; Vanderzande, D.; Huong Nguyen, L.; Neugebauer, H.; Sariciftci, S.; Aguirre, A., Low band gap donor− acceptor conjugated polymers toward organic solar cells applications. *Macromolecules* **2007,** *40* (1), 65-72.
9. Morin, J.-F.; Leclerc, M., 2, 7-Carbazole-based conjugated polymers for blue, green, and red light emission. *Macromolecules* **2002,** *35* (22), 8413-8417.
10. Donat-Bouillud, A.; Levesque, I.; Tao, Y.; D'Iorio, M.; Beaupré, S.; Blondin, P.; Ranger, M.; Bouchard, J.; Leclerc, M., Light-emitting diodes from fluorene-based π-conjugated polymers. *Chem. Mater.* **2000,** *12* (7), 1931-1936.
11. Liu, Y.; Liu, Y.; Zhan, X., High-Mobility Conjugated Polymers Based on Fused-Thiophene Building Blocks. *Macromol. Chem. Phys.* **2011,** *212* (5), 428-443.
12. Kang, I.; Yun, H.-J.; Chung, D. S.; Kwon, S.-K.; Kim, Y.-H., Record high hole mobility in polymer semiconductors via side-chain engineering. *J. Am. Chem. Soc.* **2013,** *135* (40), 14896-14899.
13. Liu, Q.; Bottle, S. E.; Sonar, P., Developments of Diketopyrrolopyrrole-Dye-Based Organic Semiconductors for a Wide Range of Applications in Electronics. *Advanced Materials* **2020,** *32* (4), 1903882.
14. Li, S.; Ye, L.; Zhao, W.; Yan, H.; Yang, B.; Liu, D.; Li, W.; Ade, H.; Hou, J., A wide band gap polymer with a deep highest occupied molecular orbital level enables 14.2% efficiency in polymer solar cells. *J. Am. Chem. Soc.* **2018,** *140* (23), 7159-7167.
15. Liu, Z.; Gao, Y.; Dong, J.; Yang, M.; Liu, M.; Zhang, Y.; Wen, J.; Ma, H.; Gao, X.; Chen, W., Chlorinated Wide-Bandgap Donor Polymer Enabling Annealing Free Nonfullerene Solar Cells with the Efficiency of 11.5%. *J. Phys. Chem. Lett.* **2018,** *9* (24), 6955-6962.
16. Yao, H.; Ye, L.; Zhang, H.; Li, S.; Zhang, S.; Hou, J., Molecular design of benzodithiophene-based organic photovoltaic materials. *Chem. Rev.* **2016,** *116* (12), 7397-7457.
17. Yang, Y.; Liu, Z.; Chen, L.; Yao, J.; Lin, G.; Zhang, X.; Zhang, G.; Zhang, D., Conjugated Semiconducting Polymer with Thymine Groups in the Side Chains: Charge Mobility Enhancement and Application for Selective Field-Effect Transistor Sensors toward CO and H2S. *Chem. Mater.* **2019**.
18. Mei, J.; Bao, Z., Side chain engineering in solution-processable conjugated polymers. *Chem. Mater.* **2013,** *26* (1), 604-615.

19. Liu, Z.; Zhang, G.; Zhang, D., Modification of Side Chains of Conjugated Molecules and Polymers for Charge Mobility Enhancement and Sensing Functionality. *Acc. Chem. Res.* **2018,** *51* (6), 1422-1432.
20. Yao, J.; Yu, C.; Liu, Z.; Luo, H.; Yang, Y.; Zhang, G.; Zhang, D., Significant improvement of semiconducting performance of the diketopyrrolopyrrole–quaterthiophene conjugated polymer through side-chain engineering via hydrogen-bonding. *J. Am. Chem. Soc.* **2015,** *138* (1), 173-185.
21. Ye, L.; Li, W.; Guo, X.; Zhang, M.; Ade, H., Polymer Side-chain Variation Induces Microstructural Disparity in Nonfullerene Solar Cells. *Chem. Mater.* **2019,** *31* (17), 6568-6577.
22. Wang, Z.; Liu, Z.; Ning, L.; Xiao, M.; Yi, Y.; Cai, Z.; Sadhanala, A.; Zhang, G.; Chen, W.; Sirringhaus, H.; Zhang, D., Charge Mobility Enhancement for Conjugated DPP-Selenophene Polymer by Simply Replacing One Bulky Branching Alkyl Chain with Linear One at Each DPP Unit. *Chem. Mater.* **2018,** *30* (9), 3090-3100.
23. Ma, J.; Liu, Z.; Yao, J.; Wang, Z.; Zhang, G.; Zhang, X.; Zhang, D., Improving Ambipolar Semiconducting Properties of Thiazole-Flanked Diketopyrrolopyrrole-Based Terpolymers by Incorporating Urea Groups in the Side-Chains. *Macromolecules* **2018,** *51* (15), 6003-6010.
24. Lobez, J. M.; Andrew, T. L.; Bulovic, V.; Swager, T. M., Improving the performance of P3HT–fullerene solar cells with side-chain-functionalized poly (thiophene) additives: a new paradigm for polymer design. *ACS Nano* **2012,** *6* (4), 3044-3056.
25. Li, Z.; Zhang, Y.; Tsang, S.-W.; Du, X.; Zhou, J.; Tao, Y.; Ding, J., Alkyl side chain impact on the charge transport and photovoltaic properties of benzodithiophene and diketopyrrolopyrrole-based copolymers. *J. Phys. Chem. C.* **2011,** *115* (36), 18002-18009.
26. Chen, M. S.; Lee, O. P.; Niskala, J. R.; Yiu, A. T.; Tassone, C. J.; Schmidt, K.; Beaujuge, P. M.; Onishi, S. S.; Toney, M. F.; Zettl, A., Enhanced solid-state order and field-effect hole mobility through control of nanoscale polymer aggregation. *J. Am. Chem. Soc.* **2013,** *135* (51), 19229-19236.
27. Lam, K. H.; Foong, T. R. B.; Ooi, Z. E.; Zhang, J.; Grimsdale, A. C.; Lam, Y. M., Enhancing the Performance of Solution-Processed Bulk-Heterojunction Solar Cells Using Hydrogen-Bonding-Induced Self-Organization of Small Molecules. *ACS Applied Materials & Interfaces* **2013,** *5* (24), 13265-13274.
28. Freudenberg, J.; Jänsch, D.; Hinkel, F.; Bunz, U. H. F., Immobilization Strategies for Organic Semiconducting Conjugated Polymers. *Chemical Reviews* **2018,** *118* (11), 5598-5689.
29. Yang, K.; He, T.; Chen, X.; Cheng, S. Z. D.; Zhu, Y., Patternable Conjugated Polymers with Latent Hydrogen-Bonding on the Main Chain. *Macromolecules* **2014,** *47* (24), 8479-8486.
30. Guo, Z.-H.; Ai, N.; McBroom, C. R.; Yuan, T.; Lin, Y.-H.; Roders, M.; Zhu, C.; Ayzner, A. L.; Pei, J.; Fang, L., A side-chain engineering approach to solvent-resistant semiconducting polymer thin films. *Polymer Chemistry* **2016,** *7* (3), 648-655.
31. Li, S.; Ye, L.; Zhao, W.; Yan, H.; Yang, B.; Liu, D.; Li, W.; Ade, H.; Hou, J., A wide band gap polymer with a deep highest occupied molecular orbital level enables 14.2% efficiency in polymer solar cells. *Journal of the American Chemical Society* **2018,** *140* (23), 7159-7167.
32. Liu, Z.; Gao, Y.; Dong, J.; Yang, M.; Liu, M.; Zhang, Y.; Wen, J.; Ma, H.; Gao, X.; Chen, W., Chlorinated Wide-Bandgap Donor Polymer Enabling Annealing Free Nonfullerene Solar Cells with the Efficiency of 11.5%. *The journal of physical chemistry letters* **2018,** *9* (24), 6955-6962.
33. Huang, Y.; Guo, X.; Liu, F.; Huo, L.; Chen, Y.; Russell, T. P.; Han, C. C.; Li, Y.; Hou, J., Improving the Ordering and Photovoltaic Properties by Extending π–Conjugated Area of Electron-Donating Units in Polymers with D-A Structure. *Adv. Mater.* **2012,** *24* (25), 3383-3389.
34. Zhang, F.; Hu, Y.; Schuettfort, T.; Di, C.-a.; Gao, X.; McNeill, C. R.; Thomsen, L.; Mannsfeld, S. C.; Yuan, W.; Sirringhaus, H., Critical role of alkyl chain branching of organic semiconductors in enabling solution-processed n-channel organic thin-film transistors with mobility of up to 3.50 cm2 V–1 s–1. *J. Am. Chem. Soc.* **2013,** *135* (6), 2338-2349.
35. McHale, R.; O'Reilly, R. K., Nucleobase containing synthetic polymers: advancing biomimicry via controlled synthesis and self-assembly. *Macromolecules* **2012,** *45* (19), 7665-7675.

36. Zhao, Y.; Sakai, F.; Su, L.; Liu, Y.; Wei, K.; Chen, G.; Jiang, M., Progressive Macromolecular Self-Assembly: From Biomimetic Chemistry to Bio-Inspired Materials. *Adv. Mater.* **2013,** *25* (37), 5215-5256.
37. Bäuerle, P.; Emge, A., Specific Recognition of Nucleobase-Functionalized Polythiophenes. *Advanced Materials* **1998,** *10* (4), 324-330.
38. Sabury, S.; Collier, G. S.; Ericson, M. N.; Kilbey, S. M., Synthesis of a soluble adenine-functionalized polythiophene through direct arylation polymerization and its fluorescence responsive behavior. *Polymer Chemistry* **2020,** *11* (4), 820-829.
39. Spada, G. P.; Lena, S.; Masiero, S.; Pieraccini, S.; Surin, M.; Samorì, P., Guanosine-based Hydrogen-bonded Scaffolds: Controlling the Assembly of Oligothiophenes. *Advanced Materials* **2008,** *20* (12), 2433-2438.
40. Navacchia, M. L.; Favaretto, L.; Treossi, E.; Palermo, V.; Barbarella, G., Self-Complementary Nucleoside-Thiophene Hybrid Systems: Synthesis and Supramolecular Organization. *Macromolecular Rapid Communications* **2010,** *31* (4), 351-355.
41. Liu, X.; Zhang, Q.; Duan, L.; Gao, G., Bio-inspired nucleobase-driven non-swellable adhesive and tough gel with excellent underwater adhesion. *ACS Appl. Mater. Interfaces* **2019,** *11* (6), 6644-6651.
42. Kim, E.; Mishra, A. K.; Choi, C.; Kim, M.; Park, S.; Park, S. Y.; Ahn, S.; Kim, J. K., Phase Behavior of Adenine-Containing Block Copolymer. *Macromolecules* **2018,** *51* (24), 10223-10229.
43. Cheng, C.-C.; Chu, Y.-L.; Huang, P.-H.; Yen, Y.-C.; Chu, C.-W.; Yang, A. C.-M.; Ko, F.-H.; Chen, J.-K.; Chang, F.-C., Bioinspired hole-conducting polymers for application in organic light-emitting diodes. *J. Mater. Chem.* **2012,** *22* (35), 18127-18131.
44. Cheng, C.-C.; Chang, F.-C.; Dai, S. A.; Lin, Y.-L.; Lee, D.-J., Bio-complementary supramolecular polymers with effective self-healing functionality. *RSC Adv.* **2015,** *5* (110), 90466-90472.
45. González-Rodríguez, D.; Schenning, A. P., Hydrogen-bonded supramolecular π-functional materials. *Chem. Mater.* **2010,** *23* (3), 310-325.
46. Bou Zerdan, R.; Cohn, P.; Puodziukynaite, E.; Baker, M. B.; Voisin, M.; Sarun, C.; Castellano, R. K., Synthesis, optical properties, and electronic structures of nucleobase-containing π-conjugated oligomers. *J. Org. Chem.* **2015,** *80* (3), 1828-1840.
47. Collier, G. S.; Brown, L. A.; Boone, E. S.; Kaushal, M.; Ericson, M. N.; Walter, M. G.; Long, B. K.; Kilbey, S. M., Linking design and properties of purine-based donor–acceptor chromophores as optoelectronic materials. *J. Mater. Chem. C* **2017,** *5* (27), 6891-6898.
48. Jatsch, A.; Kopyshev, A.; Mena-Osteritz, E.; Bäuerle, P., Self-Organizing Oligothiophene−Nucleoside Conjugates: Versatile Synthesis via "Click"-Chemistry. *Organic Letters* **2008,** *10* (5), 961-964.
49. Mishra, A.; Ma, C.-Q.; Bäuerle, P., Functional Oligothiophenes: Molecular Design for Multidimensional Nanoarchitectures and Their Applications. *Chemical Reviews* **2009,** *109* (3), 1141-1276.
50. Jatsch, A.; Schillinger, E. K.; Schmid, S.; Bäuerle, P., Biomolecule assisted self-assembly of π-conjugated oligomers. *Journal of Materials Chemistry* **2010,** *20* (18), 3563-3578.
51. Gan, K. P.; Yoshio, M.; Sugihara, Y.; Kato, T., Guanine–oligothiophene conjugates: liquid-crystalline properties, photoconductivities and ion-responsive emission of their nanoscale assemblies. *Chemical Science* **2018,** *9* (3), 576-585.
52. Cheng, C.-C.; Chu, C.-W.; Huang, J.-J.; Liao, Z.-S., Complementary hydrogen bonding interaction-mediated hole injection in organic light-emitting devices. *J. Mater. Chem. C* **2017,** *5* (19), 4736-4741.
53. Coropceanu, V.; Cornil, J.; da Silva Filho, D. A.; Olivier, Y.; Silbey, R.; Brédas, J.-L., Charge transport in organic semiconductors. *Chem. Rev.* **2007,** *107* (4), 926-952.

54. Cornil, J.; Beljonne, D.; Calbert, J. P.; Brédas, J. L., Interchain interactions in organic π-conjugated materials: impact on electronic structure, optical response, and charge transport. *Adv. Mater.* **2001,** *13* (14), 1053-1067.
55. Zhang, X.; Bronstein, H.; Kronemeijer, A. J.; Smith, J.; Kim, Y.; Kline, R. J.; Richter, L. J.; Anthopoulos, T. D.; Sirringhaus, H.; Song, K., Molecular origin of high field-effect mobility in an indacenodithiophene–benzothiadiazole copolymer. *Nat. Commun.* **2013,** *4*, 2238.
56. Lamport, Z. A.; Haneef, H. F.; Anand, S.; Waldrip, M.; Jurchescu, O. D., Tutorial: Organic field-effect transistors: Materials, structure and operation. *J. Appl. Phys.* **2018,** *124* (7), 071101.
57. Jang, W.; Cheon, H.; Park, S.; Cho, J. S.; Yi, M.; Kwon, S.-K.; Kim, Y.-H.; Wang, D. H., Interface engineering on phenanthrocarbazole/thienopyrroledione-based conjugated polymer for efficient organic photovoltaic devices with ideal nano-morphology and improved charge carrier dynamics. *Dyes Pigm.* **2017,** *145*, 29-36.
58. Chasteen, S. V.; Sholin, V.; Carter, S. A.; Rumbles, G., Towards optimization of device performance in conjugated polymer photovoltaics: Charge generation, transfer and transport in poly (p-phenylene-vinylene) polymer heterojunctions. *Sol. Energy Mater. Sol. Cells* **2008,** *92* (6), 651-659.
59. Nguyen, T.-Q.; Kwong, R. C.; Thompson, M. E.; Schwartz, B. J., Improving the performance of conjugated polymer-based devices by control of interchain interactions and polymer film morphology. *Appl. Phys. Lett.* **2000,** *76* (17), 2454-2456.
60. Lei, T.; Dou, J. H.; Pei, J., Influence of Alkyl Chain Branching Positions on the Hole Mobilities of Polymer Thin-Film Transistors. *Adv. Mater.* **2012,** *24* (48), 6457-6461.
61. Cheng, C.-C.; Chang, F.-C.; Ko, F.-H.; Yu, F.-C.; Lin, Y.-T.; Shieh, Y.-T.; Chen, J.-K.; Lee, D.-J., Supramolecular polymeric micelles as high performance electrochemical materials. *Journal of Materials Chemistry C* **2015,** *3* (37), 9528-9533.
62. Wang, B.; Zhang, W.; Zhang, W.; Mujumdar, A. S.; Huang, L., Progress in Drying Technology for Nanomaterials. *Drying Technology* **2005,** *23* (1-2), 7-32.
63. Gudarzi, M. M.; Sharif, F., Enhancement of dispersion and bonding of graphene-polymer through wet transfer of functionalized graphene oxide. *Express Polymer Letters* **2012,** *6* (12).
64. D'Addio, S. M.; Kafka, C.; Akbulut, M.; Beattie, P.; Saad, W.; Herrera, M.; Kennedy, M. T.; Prud'homme, R. K., Novel Method for Concentrating and Drying Polymeric Nanoparticles: Hydrogen Bonding Coacervate Precipitation. *Molecular Pharmaceutics* **2010,** *7* (2), 557-564.
65. Wang, Q.; Zhang, J.; Wang, A., Freeze-drying: A versatile method to overcome re-aggregation and improve dispersion stability of palygorskite for sustained release of ofloxacin. *Applied Clay Science* **2014,** *87*, 7-13.
66. Chuang, H.-Y.; Hsu, S. L.-C.; Lee, P.-I.; Lee, J.-F.; Huang, S.-Y.; Lin, S.-W.; Lin, P.-Y., Synthesis and properties of a new conjugated polymer containing benzodithiophene for polymer solar cells. *Polym. Bull.* **2014,** *71* (5), 1117-1130.
67. Hou, J.; Chen, H.-Y.; Zhang, S.; Yang, Y., Synthesis and photovoltaic properties of two benzo [1, 2-b: 3, 4-b'] dithiophene-based conjugated polymers. *J. Phys. Chem. C.* **2009,** *113* (50), 21202-21207.
68. Wang, X.; Deng, W.; Chen, Y.; Wang, X.; Ye, P.; Wu, X.; Yan, C.; Zhan, X.; Liu, F.; Huang, H., Fine-tuning solid state packing and significantly improving photovoltaic performance of conjugated polymers through side chain engineering via random polymerization. *J. Mater. Chem. A* **2017,** *5* (11), 5585-5593.
69. Lee, K. H.; Lee, H. J.; Morino, K.; Sudo, A.; Endo, T., Synthesis and Optical Properties of π-Conjugated Polymers Composed of Benzo [1, 2-b: 4, 5-b'] dithiophene and Thiophenes Bearing Electron-Deficient Ethenyl Groups in the Side Chains. *Macromol. Chem. Phys.* **2010,** *211* (23), 2490-2496.
70. Tamami, M.; Hemp, S. T.; Zhang, K. R.; Zhang, M. Q.; Moore, R. B.; Long, T. E., Poly(ethylene glycol)-based ammonium ionenes containing nucleobases. *Polymer* **2013,** *54* (6), 1588-1595.
71. Thordarson, P., Determining association constants from titration experiments in supramolecular chemistry. *Chem. Soc. Rev.* **2011,** *40* (3), 1305-1323.

72. Chen, J. S.; Shirts, R. B., Iterative determination of the NMR monomer shift and dimerization constant in a self-associating system. *J. Phys. Chem.* **1985,** *89* (9), 1643-1646.
73. Tan, H. K. S., Determination of the NMR monomer shift and dimerization constant in a self-associating system by direct application of the least-squares method. *J. Chem. Soc.-Faraday Trans.* **1994,** *90* (23), 3521-3525.
74. Zhang, K. R.; Aiba, M.; Fahs, G. B.; Hudson, A. G.; Chiang, W. D.; Moore, R. B.; Ueda, M.; Long, T. E., Nucleobase-functionalized acrylic ABA triblock copolymers and supramolecular blends. *Polym. Chem.* **2015,** *6* (13), 2434-2444.
75. Fagnani, D. E.; Zerdan, R. B.; Castellano, R. K., Synthesis, Optoelectronic Properties, Self-Association, and Base Pairing of Nucleobase-Functionalized Oligothiophenes. *J. Org. Chem.* **2018,** *83* (20), 12711-12721.
76. Benesi, H. A.; Hildebrand, J. H., A spectrophotometric investigation of the interaction of iodine with aromatic hydrocarbons. *J. Am. Chem. Soc.* **1949,** *71* (8), 2703-2707.
77. Steiner, T., The Hydrogen Bond in the Solid State. *Angewandte Chemie International Edition* **2002,** *41* (1), 48-76.
78. Hirai, T.; Nagae, Y.; White, K. L.; Kamitani, K.; Kido, M.; Uchiyama, T.; Nishibori, M.; Konishi, Y.; Yokomachi, K.; Sugimoto, R.; Saigo, K.; Ohishi, T.; Higaki, Y.; Kojio, K.; Takahara, A., Solvent free oxidative coupling polymerization of 3-hexylthiophene (3HT) in the presence of FeCl3 particles. *RSC Advances* **2016,** *6* (113), 111993-111996.
79. Rozenberg, M.; Shoham, G.; Reva, I.; Fausto, R., Spontaneous self-association of adenine and uracil in polycrystals from low temperature FTIR spectra in the range below 1000cm$^{-1}$. *Spectrochimica Acta Part A: Molecular and Biomolecular Spectroscopy* **2005,** *62* (1), 233-238.
80. Kyogoku, Y.; Higuchi, S.; Tsuboi, M., Intra-red absorption spectra of the single crystals of 1-methyl-thymine, 9-methyladenine and their 1:1 complex. *Spectrochimica Acta Part A: Molecular Spectroscopy* **1967,** *23* (4), 969-983.
81. Mathlouthi, M.; Seuvre, A.-M.; Koenig, J. L., FTIR and laser-Raman spectra of adenine and adenosine. *Carbohydrate Research* **1984,** *131* (1), 1-15.
82. Mathlouthi, M.; Seuvre, A.-M.; L. Koenig, J., FTIR and laser-Raman spectra of thymine and thymidine. *Carbohydrate Research* **1984,** *134* (1), 23-38.
83. de Jesus, J. C.; Pires, P. A. R.; Scharf, M.; El Seoud, O. A., Solvation by aqueous solutions of imidazole-based ionic liquids: 2- A comparison between alkyl and alkoxy side-chains. *Fluid Phase Equilibria* **2017,** *451*, 48-56.
84. Ajayaghosh, A.; George, S. J., First Phenylenevinylene Based Organogels: Self-Assembled Nanostructures via Cooperative Hydrogen Bonding and π-Stacking. *Journal of the American Chemical Society* **2001,** *123* (21), 5148-5149.
85. Hou, L.; Adhikari, S.; Tian, Y.; Scheblykin, I. G.; Orrit, M., Absorption and Quantum Yield of Single Conjugated Polymer Poly[2-methoxy-5-(2-ethylhexyloxy)-1,4-phenylenevinylene] (MEH-PPV) Molecules. *Nano Lett.* **2017,** *17* (3), 1575-1581.
86. Cheng, C.-C.; Chu, Y.-L.; Chang, F.-C.; Lee, D.-J.; Yen, Y.-C.; Chen, J.-K.; Chu, C.-W.; Xin, Z., New bioinspired hole injection/transport materials for highly efficient solution-processed phosphorescent organic light-emitting diodes. *Nano Energy* **2015,** *13*, 1-8.
87. Kaushal, M.; Ortiz, A. L.; Kassel, J. A.; Hall, N.; Lee, T. D.; Singh, g.; Walter, M. G., Enhancing Exciton Diffusion in Porphyrin Thin Films Using Peripheral Carboalkoxy Groups to Influence Molecular Assembly. *J. Mater. Chem. C* **2016,** *4*, 5602-5609.
88. Hou, J.; Park, M.-H.; Zhang, S.; Yao, Y.; Chen, L.-M.; Li, J.-H.; Yang, Y., Bandgap and molecular energy level control of conjugated polymer photovoltaic materials based on benzo [1, 2-b: 4, 5-b'] dithiophene. *Macromolecules* **2008,** *41* (16), 6012-6018.

89. Gonçalves, L. M.; Batchelor-McAuley, C.; Barros, A. A.; Compton, R. G., Electrochemical Oxidation of Adenine: A Mixed Adsorption and Diffusion Response on an Edge-Plane Pyrolytic Graphite Electrode. *J. Phys. Chem. C.* **2010,** *114* (33), 14213-14219.
90. Wang, Z. B.; Helander, M. G.; Greiner, M. T.; Qiu, J.; Lu, Z. H., Carrier mobility of organic semiconductors based on current-voltage characteristics. *J. Appl. Phys.* **2010,** *107* (3), 034506.
91. Dixon, A. G.; Visvanathan, R.; Clark, N. A.; Stingelin, N.; Kopidakis, N.; Shaheen, S. E., Molecular weight dependence of carrier mobility and recombination rate in neat P3HT films. *J. Polym. Sci. Part B* **2018,** *56* (1), 31-35.
92. Mohammad, L.; Chen, Q.; Mitul, A.; Sun, J.; Khatiwada, D.; Vaagensmith, B.; Zhang, C.; Li, J.; Qiao, Q., Improved Performance for Inverted Organic Photovoltaics via Spacer between Benzodithiophene and Benzothiazole in Polymers. *J. Phys. Chem. C.* **2015,** *119* (33), 18992-19000.
93. Amonoo, J. A.; Li, A.; Purdum, G. E.; Sykes, M. E.; Huang, B.; Palermo, E. F.; McNeil, A. J.; Shtein, M.; Loo, Y.-L.; Green, P. F., An all-conjugated gradient copolymer approach for morphological control of polymer solar cells. *J. Mater. Chem. A* **2015,** *3* (40), 20174-20184.
94. Collier, G. S.; Brown, L. A.; Boone, E. S.; Long, B. K.; Kilbey, S. M., Synthesis of main chain purine-based copolymers and effects of monomer design on thermal and optical properties. *ACS Macro Lett.* **2016,** *5* (6), 682-687.

## TOC Graphic

# Synthesis and Optoelectronic Properties of Benzodithiophene-Based Conjugated Polymers with Hydrogen Bonding Nucleobase Side Chain Functionality